Image Formation Mechanism of Ultra Fine Grain Emulsion BB640 Processed with High Contrast Developer D8

M. Ulibarrena, M. J. Mendez, S. Blaya, L. Carretero, R. F. Madrigal, and A. Fimia▲

Universidad Miguel Hernandez De Elche, Departamento de Ciencia y Tecnologia de Materiales, Division de Optica Avda. Ferrocarril s/n, Alicante, Spain

Photographic emulsions based on silver halide grains and their developers are characterized by the H-D curve, relating density with exposure. The H-D curve depends on a number of parameters from both of the emulsion and of the developing process, and always has a typical shape. In this study we present a H-D curve obtained with an ultra fine emulsion, Colourholographics BB640, developed with a high contrast developer, Kodak D8, whose shape differs considerably from that of the standard curve. This process leads to very high values of density as well as to an apparent holographic overmodulation. Based on these results an image formation mechanism is proposed.

Journal of Imaging Science and Technology 47: 69–77 (2003)

Introduction

Of the materials suitable for holographic recording, fine and ultra-fine grain silver halide emulsions have the highest light sensitivity. The photographic and holographic properties of silver halide emulsions are the best known of all high resolution materials, since these emulsions have been deeply studied and used for more than a century.[1–5] In recent years, due to fact that the historical manufacturers of fine and ultra fine grain emulsion discontinued production of these materials, new emulsions of this kind have appeared on the market. These new emulsions have new characteristics and, therefore, different photographic and holographic properties compared to the discontinued emulsions.

The characteristics of Colourholographics BB640[6] emulsions studied in this work differ from those of older emulsions in such important features as thickness of the layer (between 7 and 9 μm for BB640 compared with ≤6 μm for Agfa 8E and Ilford and 12 μm for Kodak 649F), mean grain size (20 nm for BB640 against 40 nm for the other emulsions mentioned), sensitivity, and hardness of the supporting gelatin.[7,8] We assume that these differences may be related to the results reported in this article. These results were not found with the earlier emulsions in all the years they were used for holographic applications or as high resolution photographic materials.

BB640 emulsions have been recently studied as holographic recording materials using conventional fine grain processing schemes commonly used with the classical emulsions. The results reported are not very different from those of the discontinued emulsions.[9]

The most important difference that we found when working with BB640 plates is related to the anomalous D-Log E curve[10] obtained when processing BB640 emulsion with Kodak D8,[11] a high contrast developer rarely used in holography,[12] and whose properties have been photographically analyzed.[13] The special characteristics of Kodak D8 developer are the following:

- It works at a very high pH value (>13) but it is not a buffered solution, although it includes a strong base (NaOH) to raise the pH. Since no buffer is present, we can expect local pH changes as the development process takes place, thus leading to an important local and time dependence of the development process.
- Sodium sulfite, a common developer preservative, is present in a high concentration in the developer solution. But sodium sulfite is also known as a strong ultra-fine silver grain solvent, especially with BB640 plates with an average grain diameter of 20 nm.

Our own hypersensitivity studies with sodium sulfite plus urea revealed a decrease in sensitivity caused by the silver grain solution, while this was not the case for classical Agfa emulsions (average grain diameter of 40 nm) where this process increased the sensitivity by a factor of 2.[14]

The H-D curve relates the density (D) of the developed emulsion to exposure (E)[15] and is a means of characterizing photographic emulsions and their processing Density D is defined as $D = -\log T$, where T is the transmittance or transparency of the developed recording, calculated as the ratio of transmitted to incident light intensity.[1]. E is the product of the recording light intensity (I) and the exposure time (t), $E = It$.

A new feature found with these plates and this particular process is an apparent holographic overmodulation performance of the bleached gratings. Two peak values of diffraction efficiency (DE) at two different ex-

Original manuscript received March 15, 2002

▲ IS&T Member

*Corresponding author telephone: 34-96-6658428; Fax: 34-96-6658602; E-mail: m.ulibarrena@umh.es

©2003, IS&T—The Society for Imaging Science and Technology

posures separated by a low *DE* zone were found. Overmodulation typically presents this type of results and is usually found in those materials that verify that the product of thickness of the layer (d) and index modulation (n_1), which we will refer to as *optical path modulation – OPM* = $n_1 \times d$, may vary within a range wide enough for the diffraction efficiency to reach its first maximum value, decreasing to a minimum, reach its next maximum value and so on periodically. According to Kogelnik's coupled wave theory,[16] this behavior continues until a certain limit of *OPM* for the material is reached. *DE* in the case of an unslanted lossless transmission grating recorded in a material with high index modulation capability and sufficient thickness will increase and decrease periodically with the OPM according to:

$$DE = T_{sfa} \sin^2\left(\frac{\pi n_1 d}{\lambda \cos\theta}\right) \quad (1)$$

where λ is the wavelength, θ is the Bragg angle of the grating and T_{sfa} is a factor that takes into account scattering, absorption and Fresnel losses. This theoretical result has been experimentally confirmed for materials such as dichromated gelatin,[17] silver containing porous glasses[18] or photopolymers.[19] These materials may have compositions with a greater product of index modulation and thickness than the optimal one for achieving the highest possible *DE*.

Silver halide holographic materials have a relatively limited capacity for index modulation, based on the relatively small silver ion concentration present in the emulsion. This property, together with a fixed thickness determined by the manufacturers—which is never more than 12 μm—has made holographic overmodulation difficult to observe with these materials. Furthermore, the solvent action of developing agents in the presence of high concentrations of metallic silver tends to produce a decrease in local density in the exposed zones (bright zones of the interference pattern), an effect known as solarization. On the other hand, silver halide grains in the dark (unexposed) zones continue their spontaneous reduction process to give metallic silver, thereby increasing its concentration and, consequently, its local density. Thus, together with high exposure energies, changes in silver population in both zones lead to a net decrease in density modulation in the emulsion. In this case, when metallic silver is converted back into ionic silver by means of a direct bleaching process, a corresponding decrease in index modulation of the bleached plate is obtained, resulting in a diminished *DE* of the resulting hologram.

One of the key characteristics related to ultra fine grain silver halide materials used in holography is their ability to accurately store the optically generated sinusoidal interference pattern of the hologram as density differences. In order to assure this result, the linear zone of the D-Log E curve has been commonly used. When the idea of diffusion mechanisms associated with certain bleaching techniques was introduced,[3] holographers started to move towards the saturation region of the D-Log E curve. The main problem introduced by this technique is that the material response is no longer linear, leading to some distortion from the original sinusoidal profile. These distortions can be analyzed by means of the angular response of the recordings and generally appear as an asymmetric response.[20,21]

In this study we used post-development processes which are characterized by their direct action. By this we mean that they act only locally and no diffusion processes are involved. Direct bleaching is a two step process. First, the fixing step dissolves all unexposed silver halide remaining in the emulsion, thus ideally leaving only metallic silver suspended in the supporting gelatin in the bright zones of the recorded interference pattern, and only gelatin in the dark ones. The action of the direct bleach is to rehalidized the resulting silver grains, thereby generating a new silver salt. This gives rise to zones with a high concentration of silver salts inside the supporting gelatin and zones with only gelatin, so each zone will have a different refractive index. Therefore, this process directly converts the density recording into a phase recording and the density modulation into a refractive index modulation.

The second bleaching technique used in this study was reversal bleaching. In this process all metallic silver present in the emulsion is dissolved, leaving only the original unexposed and undeveloped silver halide grains. Therefore the exposed regions of the plate end up with a low concentration of silver halide crystals, whereas in the unexposed regions the original concentration is maintained. As before, no diffusion processes are associated with this bleaching technique. It must be noted that some ripening resulting in a slight increase in the original grain size, has been reported.[3] Index modulation in this case results from the different silver halide concentrations in the exposed (low concentration) and unexposed (high concentration) regions.

So with these processes we assume a direct relationship between density modulation of the developed plate and refractive index modulation of the bleached hologram. Based on this premise we will extend our density study to the results obtained from the analysis of the properties of the holographic gratings post-processed as described. Diffraction efficiency is one of the most important parameters studied, since it is directly related to index modulation. It is defined as the ratio of diffracted to incident light intensity of the probe beam at the Bragg angle. Another important tool to analyse the holographic properties, directly related to the *OPM,* is the angular response of the gratings, which consist of measuring the diffraction efficiency for different angles of incidence of the reconstructing beam. Off-Bragg diffraction efficiency provides information on the OPM of the recording.[22]

Experimental

Silver halide materials were used to record holographic unslanted transmission gratings with a spatial frequency of 1150 lp/mm with a p-polarised He-Ne laser (λ = 633 nm). Gratings were recorded in a symmetrical layout with two collimated laser beams at an angle of 21.0° to the perpendicular of the plate. A diagram of this setup is shown in Fig. 1. The beam ratio of holographic exposures was 1:1 and the power of the exposure beams was about 130 μW/cm² each. Plates were prewashed in a 3% solution of tri-ethanolamine (TEA) in deionized water for 15 minutes and dried with warm air prior to exposure. After exposure they were processed with Kodak D8 developer and fixed with non-hardening fixer Kodak F-24[11] as described in Table I. After measuring the densities, the plates were bleached with direct ferricianide bleach (potassium ferricianide, 8 g/l, and potassium bromide, 7 g/l) or Kodak R9[11] reversal bleach (fixation-free) according to Tables II and III. A reference test with plates developed with AAC (ascorbic acid, 18 g/1, and sodium carbonate, 60 g/1, for 4 minutes at 20°C) and fixed with Kodak F-24 was done in order to compare our results with a standard D-Log E curve.

TABLE I. Emulsion processing.

Kodak developer D8	4 minutes	20°C
Washing	10 minutes	
Fix with F-24	5 minutes	
Final washing	15 minutes	
Drying	room temperature	

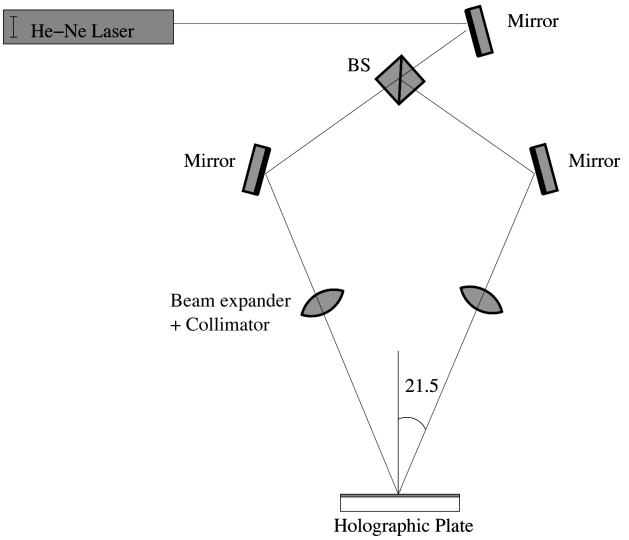

Figure 1. Interferometric setup for recording holographic transmission gratings with a spatial frequency of 1200 lp/mm.

Densities were calculated from transmission measurements taken with a solid state detector ranging from 20 W/cm^2 to 0.0001 nW/cm^2. The probe beam was a slowly expanded laser beam with an intensity of over 20 mW/cm^2. With this configuration it is not possible to measure transmission values corresponding to densities higher than 11.3, so all graphics will show that limit. Accordingly, transmission values of 0.0000 nW/cm^2 were measured, indicating higher densities outside the limits of our detector.

DE measurements of the bleached recordings were made using a collimated He-Ne laser beam at the Bragg angle of the grating. Detectors were placed 50 cm away from the plate in order to avoid the scattered radiation of the grating on the detector, to obtain indirect information on hologram quality. Angular responses of the bleached holograms were measured with a computer controlled rotating stage with steps of 0.5°. All experimental values were corrected for reflection losses based on both experimental measurements and Fresnel formulae calculations,[23] in order to avoid, especially in the angular responses, mismatches due to different angles of incidence. For this calculations we took 1.523 as the refractive index of glass and 1.579 as that of gelatin. Both values were calculated from interferometric data obtained using a thin film resonance method.[24]

Results

Transmission measurements of the unbleached plates developed with Kodak D8 resulted in the D-Log *E* curve shown in Fig. 2, which clearly differs from a typical H-D curve. Apart from the shape, which is completely different to that of a standard curve such as that obtained

TABLE II. Rehalogenating Bleaching.

Potassium ferricianide bleach	30-60 minutes*	20°C
Final washing	15 minutes	
Drying	room temperature	

* Bleaching time ranged from 30 to 60 minutes according to the higher density recording in each plate.

TABLE III. Reversal Bleaching (Fixation Free).

Kodak R-9 bleach	30-60 minutes*	20°C
Final washing	15 minutes	
Drying	room temperature	

* Bleaching time ranged from 30 to 60 minutes according to the higher density recording in each plate.

with the reference developer AAC, as shown in the same figure for comparison purposes, the most remarkable feature is the maximum density attained, which is higher than our detection limit of 11.3. Sensitivity is also higher for D8 than for AAC. The other special characteristic is that three distinct zones can be observed in the curve, labeled as region **I** ranging from exposures of 10 μJ/cm^2 to 90 μJ/cm^2, region **II** from 100 μJ/cm^2 to 400 μJ/cm^2 and region **III**, from 500 μJ/cm^2 to 7000 μJ/cm^2. Region **I,** starting at fog density and reaching a density value of 5 may be considered a standard H-D curve. The curve then reaches a low gradient zone in region II. In region **III** the D-Log *E* curve again has a steeper slope, and instead of entering the expected solarization region, the reduction process is reactivated and the limit density of 11.3 is reached. Finally, there is a gradual decrease in density.

The *DE* versus *E* curves shown in Fig. 3, together with the D-Log *E* curve, correspond to direct bleached (ferricianide) and to R-9 reversal bleached plates. Direct bleached emulsions show an apparent holographic overmodulation. We use the term *apparent holographic overmodulation* since two maximum *DE* values separated by a low *DE* zone is observed. In the reversal bleaching process, as was to be expected, the *DE* increases until it reaches a maximum and then decreases. It is remarkable that the values of exposure energy corresponding to the maximum *DE* for reversal bleach are located in zone **II,** in the energy range with low *DE* between the two maxima of the rehalogenation bleach processing.

The results obtained from the angular *DE* curves are shown in the set of figures labeled Fig. 4. We chose twelve curves from the complete set of gratings recorded, processed with D8 and post-processed with the F-24 and ferricianide direct bleach. Curves 4b and 4k correspond to the two *DE* maxima of the *DE-E* curve, and have a regular shape. Curves 4d to 4j correspond to energy region **II,** and show lower peak values for maximum *DE,* a reconstruction angle different to the recording one, and a non-symmetrical response with respect to the Bragg angle. The deviation is more dramatic in 4f, whose maximum *DE* value lies at a Bragg angle of 41°, given the recording angle of 21.0°. The second maximum *DE* is higher and slightly broader than the first one, and the maximum *DE* angle has shifted from 21.0° to 23.0°.

In order to confirm that we have obtained a holographic overmodulation response, we checked to see if these angular responses matched the theoretical results. We fitted and simulated the theoretical angular responses of

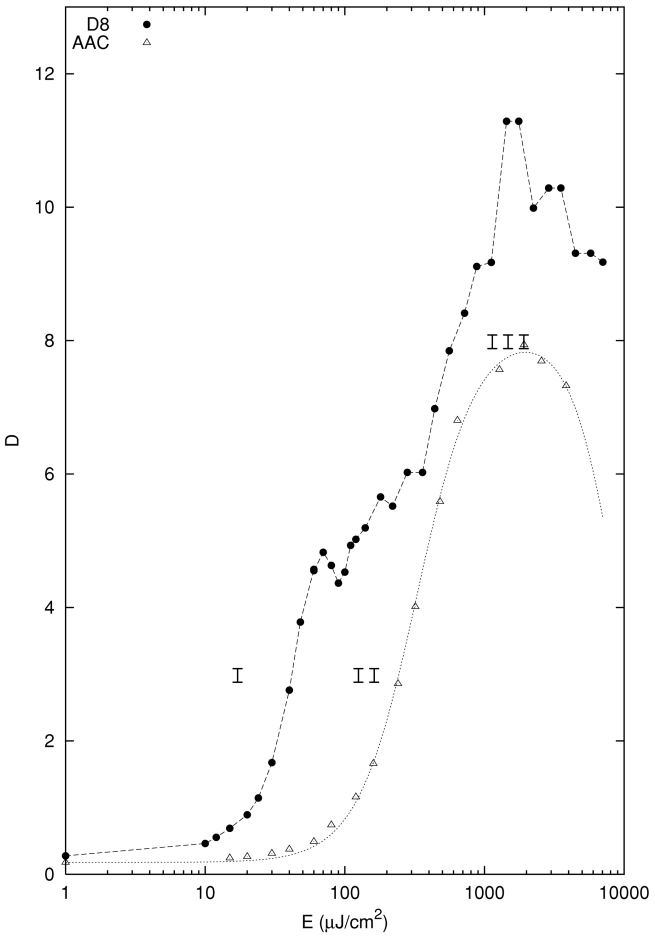

Figure 2. D–Log E curve of BB640 plates developed with Kodak D8, compared to standard D–Log E curve of same plates developed with AAC.

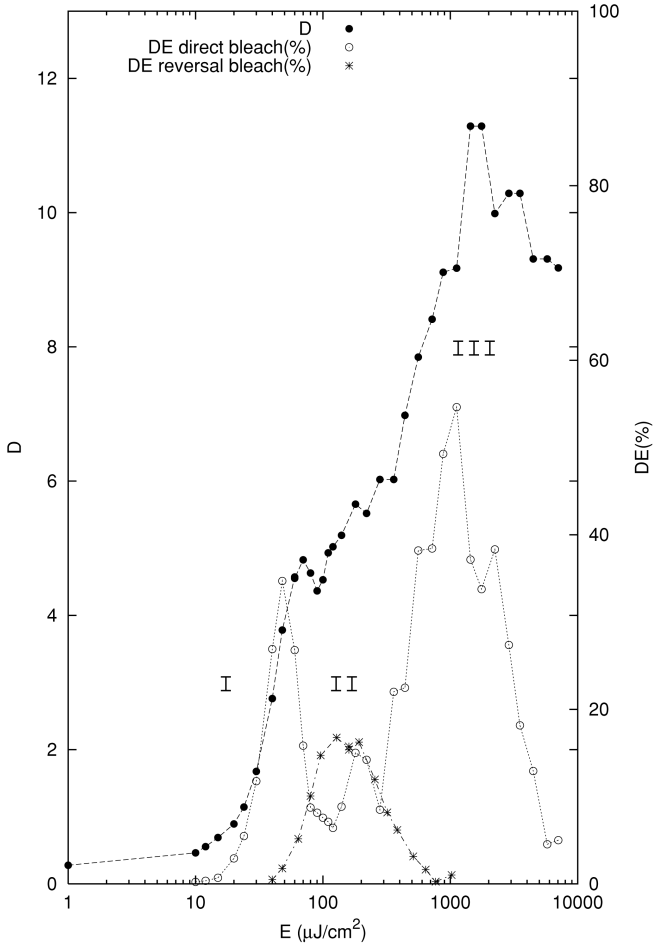

Figure 3. BB640 plates processed with Kodak D8 developer. D-Log E curve (•), *DE* - Log *E* curve for non-hardening fix followed by ferricianide rehalogenating bleaching (•) and *DE* - Log E curve for Kodak R-9 reversal bleaching (*).

holographic gratings with increasing index modulation n_1. Simulations were done, as a first approximation, according to Kogelnik's coupled wave theory[16] for an unslanted transmission grating. This model assumes that the modulation index is not attenuated in the direction perpendicular to the grating vector and that there is no bending or distortion of the generated fringes. Therefore, the expression for the off-Bragg diffraction efficiency obtained by Kogelnik is given by Eq. (2),[25]

$$\eta = T_{sfa}\frac{\sin^2\left(\sqrt{\left(\frac{\pi n_1 d}{\lambda\cos\theta}\right)^2+\left(\frac{2\Delta\theta\pi n_0 d\sin(\theta)^2}{\lambda}\right)}\right)}{1+\left(\frac{\Delta\theta n_0\sin(2\theta)}{n_1}\right)^2} \quad (2)$$

where θ is the Bragg angle at the reading wavelength (633 nm), Δθ is the angle of incidence with respect to the Bragg angle, λ is the wavelength, n_0 is the mean refractive index, n_1 is the index modulation, d is the emulsion thickness. Scattering is given by the factor, T_{sfa}, the higher that value the lower the scattered light.

Starting values for these simulations were taken from the analytical fitting calculated for the angular response curve of the first *DE* maximum, corresponding to an exposure energy of 60 μJ/cm², which lies in the first linear region of the D-Log E curve where a fairly regular response was found. Fittings were carried out using the Levemberg–Marquardt method.[26] Calculations resulted in a good fitting with a regression coefficient r^2 of 0.990 showing, for a Bragg angle of 21.0°, a modulation index n_1 of 0.049, an effective thickness of 6.79 μm and a scattering coefficient of 0.40. Figure 5 shows the comparison of the fitted curve with the experimental data. With these values we have made a set of simulations corresponding to increasing values of n_1, ranging from values lower than the fitted ones to values higher than those corresponding to the second *DE* maximum. The results are shown Fig. 6.

Discussion

When comparing the set of experimental angular responses in Fig. 4 with the set of simulated angular responses in Fig. 6, we obtained a very good fitting for experimental and theoretical values for the angular response curves of the first *DE* values. However, regarding the experimental data obtained for energy values between the two *DE* maxima (Figs. 4(d) to 4(j) and 6(d) to 6(j)), the disagreement is evident. Where the theoretical overmodulation curves indicated that we should

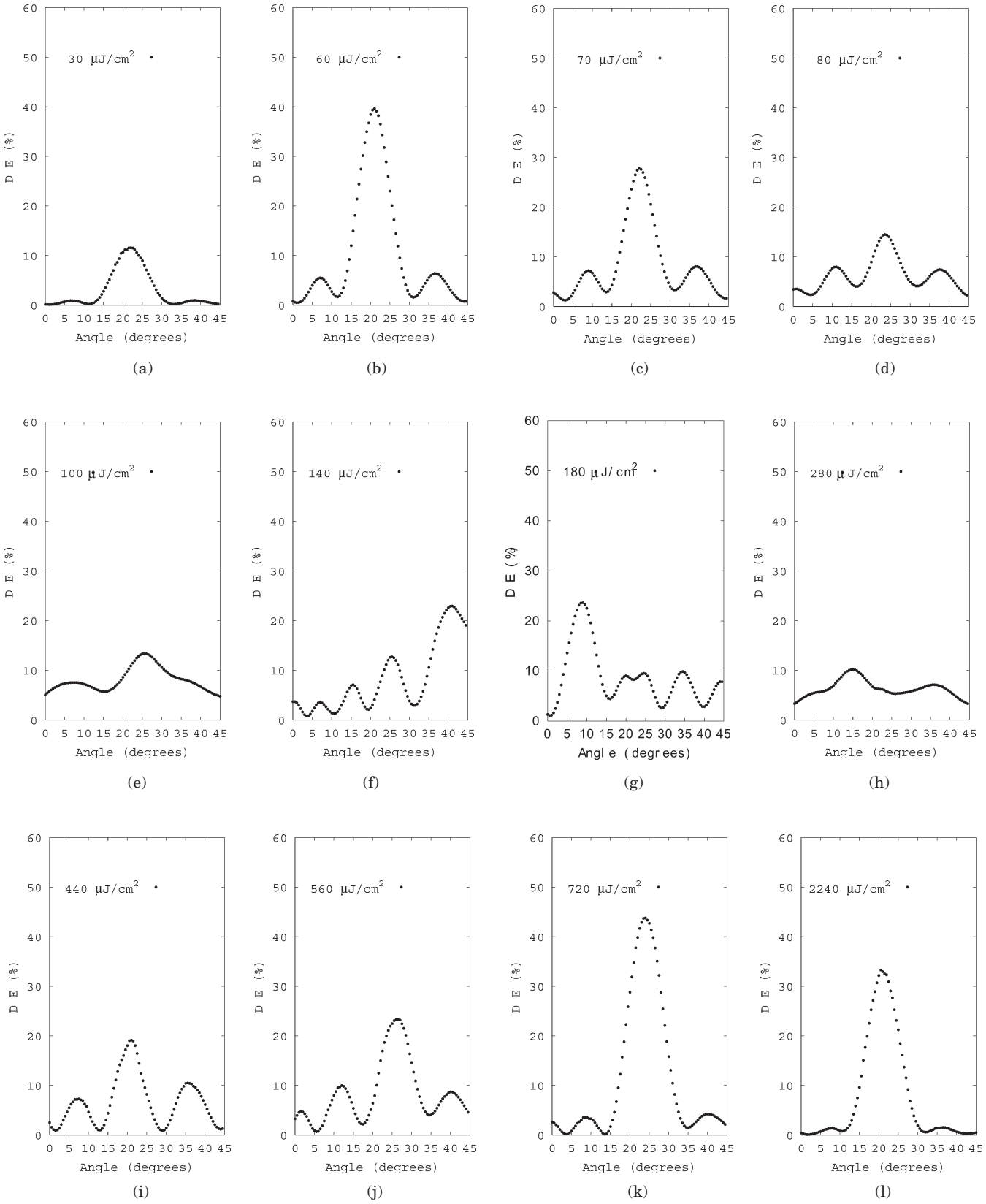

Figure 4. Angular responses of transmission gratings recorded on BB640 plates with a spatial frequency of 1200 lp/mm, processed with D8 and direct bleaching scheme.

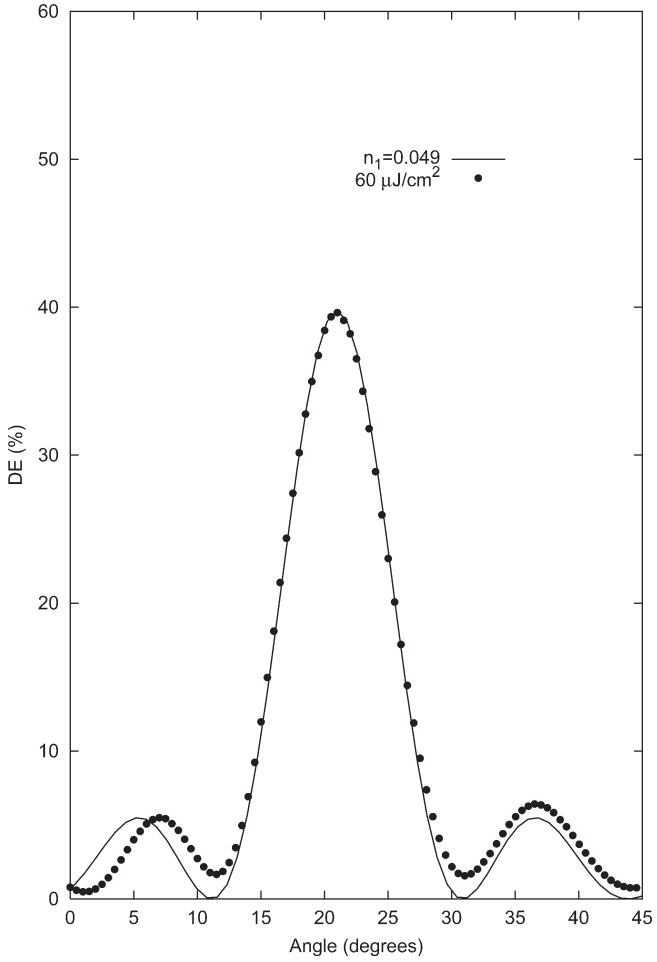

Figure 5. First *DE* maximum of direct bleached gratings recorded on BB640 plates processed with D8 and direct bleaching scheme and analytical fitting.

obtain a symmetrical angular response in relation to the Bragg angle, we found nothing of the kind in the experimental data. Furthermore, in the experimental data there is no local or absolute maximum or minimum *DE* value at the Bragg angle, as predicted by theory. Regarding the second *DE* maximum, Figs. 4(k) and 6(k), we notice some differences between them, such as the broad response and the high *DE* side lobules predicted by theory, but which were not found in the experimental angular response curves.

Based on these premises, we affirm that we are not looking at a real but an apparent overmodulation. Let us now analyze the results outlined in Fig. 3. In region I we have a linear response in the D-Log *E* curve and the first *DE* maximum value. Also it is in this region that the only good theoretical fitting for the experimental angular responses is found, and the Bragg angle is strictly maintained. Figure 7(a) represents the metallic silver and silver ion population inside the emulsion in this case. The sinusoidal profile generated by the interferometric setup is linearly reproduced by the emulsion, as expected, since we are in a linear response zone of the D-Log *E* curve.

In region **II** there is a gradual increase in *D* with *E*, and in this region we find the greatest mismatches between experimental and theoretical values for the angular responses. Since we have ruled out the existence of over modulation, we shall take into consideration an important adjacency effect.[2,27] This effect has been studied for photographic image edges using photographic emulsions with a mean grain size ranging from 350 to 1000 nm and within distances as small a 200 μm. In simple terms, the effect can be explained by diffusion of development inhibiting or retarding products from the reduction processes which accumulate in the high density zones, acting on the fresh chemical species diffusing throughout the emulsion. This effects causes edges to sharpen. In our case we are working with ultra-fine grain holographic emulsions with mean grain size of around 20 nm and the frequency of our sinusoidal interferometric patterns is 1200 lp/mm. The densities measured are an average of those local density levels. Adjacency effects result in an almost null net average density increase for the first *E* values in zone **II.**

The adjacency effect is presented in Figs. 7(b) and 7(c) at two different stages. In 7(b) the adjacency effect starts, sharpening the edges of the sinusoidal pattern. In 7(c), corresponding to a higher *E,* the high contrast developer also starts its solvent action in the presence of a high metallic silver concentration; therefore some silver ions appear in the exposed region. These ions are joined by those coming from the unexposed zones, and when there are enough of them the reduction process starts again. This results in a deformation of the profile, as shown in Fig. 7(d). This profile is the one that renders the second maximum *DE* peak in zone **III,** corresponding to the almost regular angular response shown in Fig. 4(k). The mismatch between Bragg angles in this case is caused by some deformation of the sinusoidal profile resulting from these nonlinear chemical processes, since Kogelnik's theory is valid for sinusoidal profiles only. Diffusion processes in holography have only been reported with fixation free rehalogenating bleaches,[3] but we consider that, due to the strong action of the developer, these mechanisms may apply in this case to the developing process. The profile shown in Fig. 7(d) with no silver halide left renders a 50% *DE* and an absorption coefficient of 42% corresponding to oxidation products that remain inside the emulsion after final washing. Scattering is very low, compared to that in region **II.** From this result we infer that the density modulation of the unbleached emulsion is significant, and from the D-Log *E* curve we know that it has an average density over 11.3. Consequently, local densities in the bright zones of the interferometric pattern must be even higher than this value.

It must be mentioned that these diffusion processes cause the developer to act as a kind of fixer. This 'fixing' action is not like that of a conventional fixer that dissolves silver halide grains in the fixing solution, thus removing them from the emulsion, but in the sense that there are no silver ions left since all of them are reduced by the developer. The high activity developer makes the silver ions from the silver halide crystals, under the influence of the solvent action of sulfite, diffuse towards the zone with a high silver concentration, where by a catalytic reaction they are reduced by the developer. Accordingly, practically all the silver present in the unexposed emulsion is reduced, none is dissolved, and this explains the very high densities reported.

There is further evidence about the action of the developer in the range of energies corresponding to region **II.** Figure 3 shows the *DE* curve of the solvent (reversal) bleach process. As already mentioned in the introduction of this study, this process uses only the

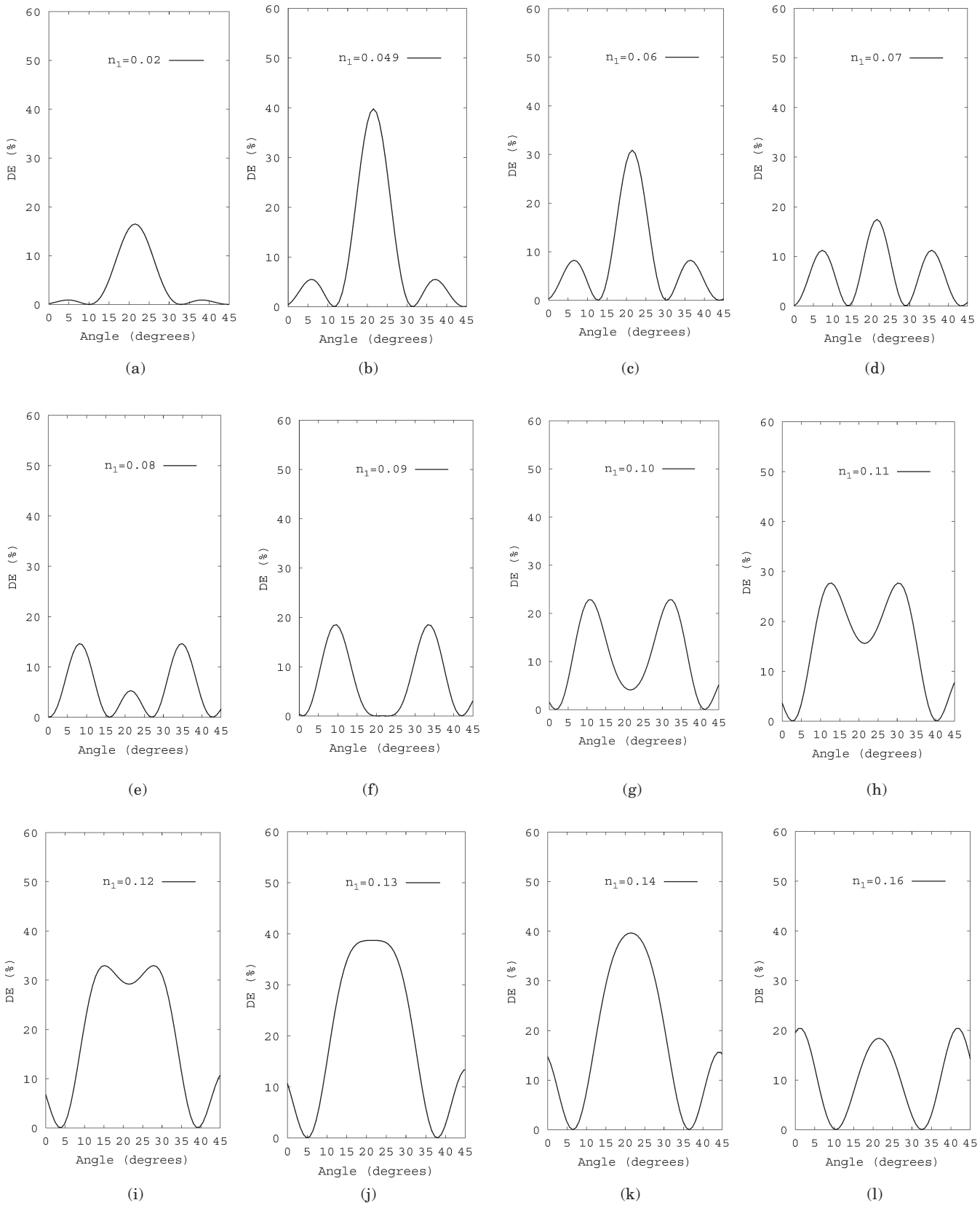

Figure 6. Simulated angular responses of transmission gratings with spatial frequency of 1200 lp/mm, effective thickness of 6.62 μm and T_{sfa} of 0.39, for a set of increasing index modulation value.

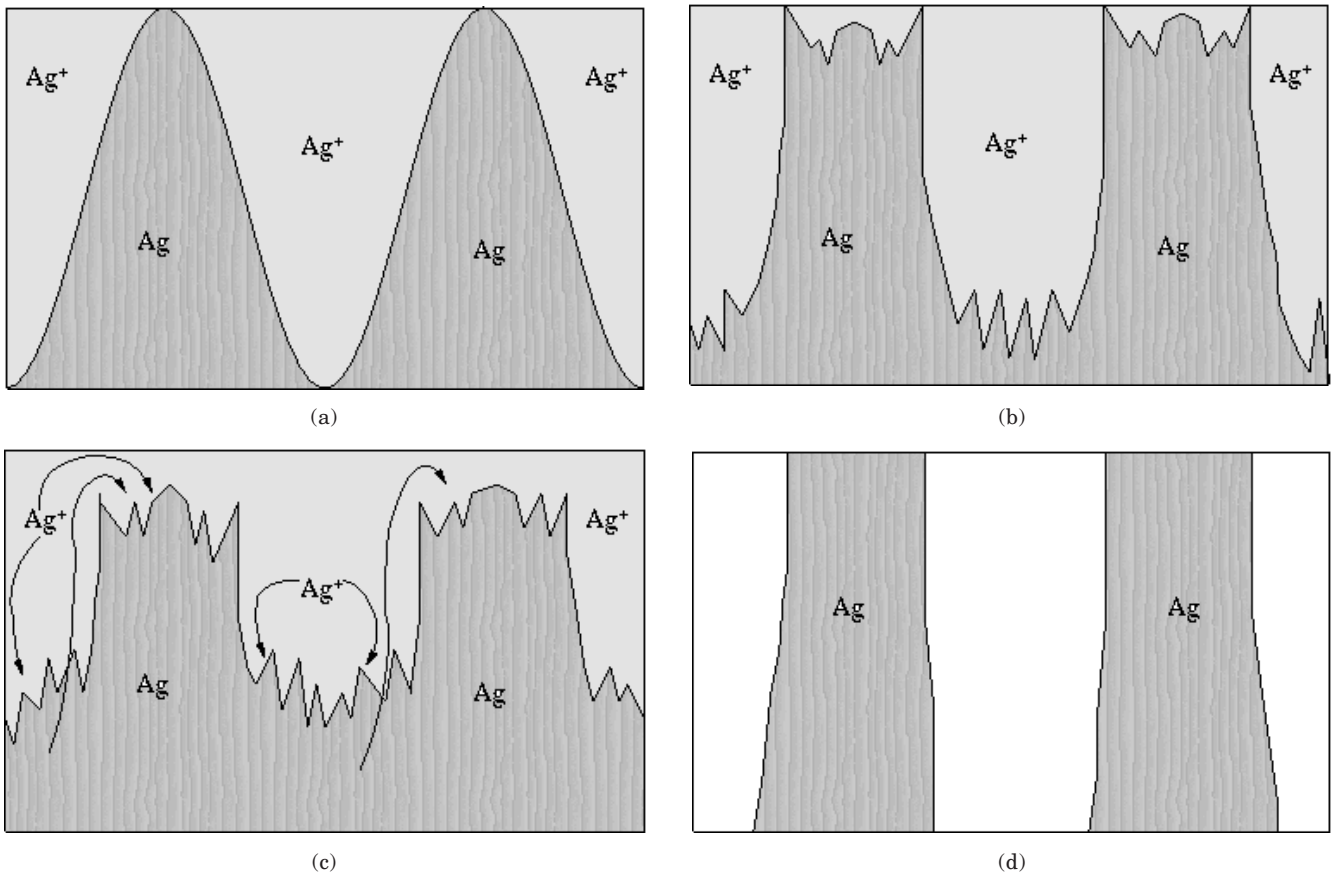

Figure 7. Proposed image formation mechanism of developer D8 acting on a high frequency interferometric sinusoidal profile recorded on BB640 plates.

original silver halide grains present in the emulsion, since it dissolves all the reduced metallic silver in the exposed zones. Index modulation is caused by the number of these crystals. At low exposure levels, the exposed zone has a low concentration of reduced silver, so that when the bleach acts, the difference of concentrations of silver halide grains between bright and dark zones of the interferometric pattern is low, resulting in a low *DE* value. On the other hand, at high exposure levels, there are few silver halide grains left in the emulsion, since most of them have been reduced by the developer, and after bleaching, the differential concentration between bright and dark zones is again small. At the optimal exposure level, we found the optimal silver halide concentration differential, and the *DE* for this energy is maximum. This maximum *DE* for this process lies in region **II,** where there is only a small net increase in *D*. However, the differential population of silver halide grains between exposed and unexposed zones rises to a maximum, therefore indicating some changes in the silver ion population. On the other hand, in region **II,** we find the zone with the lowest *DE* for the direct bleach process. Therefore, we have an undistorted sinusoidal profile for the silver halide grains (solvent bleach) for the same *E* values where we find a heavily distorted distribution of the developed silver grains.

These results, together with the fact that *D* barely increases in this region, insofar as *D* is proportional to the amount of metallic silver, indicate the existence of diffusion processes and changes in the metallic silver population and grain size (an increase in number and decrease in size) rather than the expected increase only in the number of developed grains, which would result in a faster, and continuous increase of *D*.

Conclusions

We have proposed an image formation mechanism with ultra fine grain emulsions BB640 from Colourholographics Ltd. when processed with high contrast developer Kodak D8. This mechanism involves a dramatic adjacency effect as well as diffusion mechanisms within the emulsion layer owing to the special characteristics of the developer. An apparent holographic overmodulation has been reported as well as density values higher than 11.3. These facts, together with the analysis of the angular responses of the bleached holographic recordings, have helped us to understand these mechanisms. These features may be of great interest for understanding image formation mechanisms with ultra fine grain emulsions developed with high contrast developers, which can also be employed for photolithographic applications and high contrast imaging.

References

1. C. E. K. Mees and T. H. James, *The Theory of the Photographic Process,* 3rd ed., Macmillan Co., New York, 1966.
2. J. C. Dainty and R. Shaw, *Image Science,* Academic Press, London, 1974.
3. H. I. Bjelkhagen, *Silver Halide Recording Materials,* Springer-Verlag, New York, 1993
4. Y. N. Denisyuk, Holography for Artistic Purposes with Three-dimensional Recording and Lippmann Plates, *Sov. Phys. Tech. Phys* **23**(8), 954–957 (1978).

5. N. J. Phillips, H. Heyworth, and T. Hare, On Lippmann Photography, *J. Photographic Sci.* **32,** 158–169 (1984).
6. Note. Plates type BB640 and BB520 formerly manufactured by HRT-Gmbh of Germany, are currently beeing manufactured by Colourholographics Ltd. of England.
7. S. Blaya, L. Carretero, R. F. Madrigal, and A. Fimia, Photosensitive Materials for Hologram Recording, in *Handbook of Advanced Electronic and Photonic Materials and Devices,* vol. 7, Academic Press, 2001.
8. R. Birenheide, The BB emulsion series: Current standing and future developments, in *Practical Holography,* SPIE Press, Bellingham, WA, 1997, pp. 28–30.
9. C. Neipp, I. Pascual and A. Belendez, Optimization of a Fixation-free Rehalogenating Bleach for BB640 Holographic Emulsion, *J. Modern Optics* **7(10),** 1671-1679 (2000).
10. M. Ulibarrena, M. Mendez, S. Blaya, and A. Fimia, Anomalous D-Log E Curve with High Contrast Developer Kodak D8 on Ultrafine Grain Emulsion BB640, *Optics Express*, **9,** 645–651 (December 2001).
11. Black-and-White Processing Using KODAK Chemicals, Eastman Kodak Company, Rochester, NY, 1985.
12. A. Fimia, M. Pardo and J. A. Quintana, Improvement of Image Quality in Bleached Holograms, *Appl. Opt.* **21,** 3412–3413 (1982).
13. M.R.V. Sahyun, Relationship Between Kinetics of Development of a Silver Halide Photographic Material and its Quantum Efficiency, *Photogr. Sci. Eng.* **19,** 38–43 (1975).
14. J. Crespo, A. Fimia, and J. A. Quintana, Fixation–free Methods in Bleached Reflection Holography, *Appl. Opt.* **25**(10), 1642–1645 (1986).
15. F. Hurter and V. C. Driffield, Photochemical Investigations and a New Method of Determination of the Sensitiviness of Photographic Plates, *J. Soc. Chem. Ind.* **9,** 455 (1890)
16. H. Kogelnik, Coupled Wave Theory for Thick Hologram Gratings, *Bell System Tech. J.* **48**(9) 2909–2945 (1969).
17. B. J. Chang and C. D. Leonard, Dichromated Gelatin or the Fabrication of Holographic Optical Elements, *Appl. Opt.* **18**(14), 2407–2417 (1979).
18. O. V. Andreeva, Y. L. Korzinin, V. N. Nazarov, E. R. Gavrilyuk, and A. M. Kursakova, Diffraction Efficiency of Silver-containing Holograms on Porous Glasses in the Red and IR Regions of the Spectrum, *J. Opt. Technol.* **64**(4), pp. 396–399, 1997.
19. S. Blaya, L. Carretero, A. Fimia, R. Mallavia, R. Madrigal, R. Sastre, and F. Amat-Guerri, Optimal Composition of an Acrylamide and N.N'-Methylenebisacrylamide Holographic Recording Material, *J. Modern Opt.* **45**(12), 2573-2584 (1998).
20. N. Uchida, Calculation of Diffraction Efficiency in Hologram Gratings Attenuated Along the Direction Perpendicular to the Grating Vector, *J. Opt. Soc. Amer.* **63,** 280–287 (1973).
21. T. Kubota, The bending of interference fringes inside a hologram, *Optica Acta* **26**(6), 731–743 (1979).
22. L. Garretero, R. F. Madrigal, A. Fimia, S. Blaya, and A. Belendez, Study of Angular Responses of Mixed Amplitude-phase Holographic Gratings: Shifted Borrmann Effect, *Opt. Lett.* **26,** 786–788 (2001**).**
23. M. Born and E. Wolf, *Principles of Optics,* 6th ed., Pergamon Press, London, 1983.
24. H. D. Tholl, M. Dohmen and C. G. Stojanoff, Determination of the Mean Refractive Index and the Thickness of Dichromated Gelatin Holographic Films Using the Thin Film Resonance Method, *Proc. SPIE* **2405,** 76–87 (1995).
25. S. Blaya, L. Carretero, R. Mallavia, A. Fimia, and R. F. Madrigal, Holography as a Technique for the Study of Photopolimerization Kinetics in Dry Polymeric Films with a Non Linear Response, *Appl. Opt.* **38,** 955–962 (1999).
26. S. Wolfram, *The Mathematica Book,* 4th ed., Wolfram Media, Redwood, California, 1999.
27. C. N. Nelson, Prediction of Densities in Fine Detail in Photographic Images, *Photogr. Sci. Eng.* **15,** 83–97 (1971).